The Journal of Neuroscience, November 15, 1998, *18*(22):9153–9162

A Ca^{2+}/Calmodulin-Dependent Protein Kinase Modulates *Drosophila* Photoreceptor K^+ Currents: A Role in Shaping the Photoreceptor Potential

Asher Peretz,[1,2] **Ilane Abitbol,**[1] **Alexander Sobko,**[1] **Chun-Fang Wu,**[2] **and Bernard Attali**[1]

[1]*Neurobiology Department, Weizmann Institute of Science, Rehovot 76100, Israel, and* [2]*Department of Biological Sciences, University of Iowa, Iowa City, Iowa 52442*

Light activation of *Drosophila* photoreceptors leads to the generation of a depolarizing receptor potential via opening of transient receptor potential and transient receptor potential-like cationic channels. Counteracting the light-activated depolarizing current are two voltage-gated K^+ conductances, I_A and I_K, that are expressed in these sensory neurons. Here we show that *Drosophila* photoreceptors I_A and I_K are regulated by calcium–calmodulin (Ca^{2+}/calmodulin) via a Ca^{2+}/calmodulin-dependent protein kinase (CaM kinase), with I_K being far more sensitive than I_A. Inhibition of Ca^{2+}/calmodulin by *N*-(6 aminohexyl)-5-chloro-1-naphthalenesulfonamide or trifluoperazine markedly reduced the K^+ current amplitudes. Likewise, inhibition of CaM kinases by KN-93 potently depressed I_K and accelerated its C-type inactivation kinetics. The effect of KN-93 was specific because its structurally related but functionally inactive analog KN-92 was totally ineffective. In *Drosophila* photoreceptor mutant Sh^{KS133}, which allows isolation of I_K, we demonstrate by current-clamp recording that inhibition of I_K by quinidine or tetraethylammonium increased the amplitude of the photoreceptor potential, depressed light adaptation, and slowed down the termination of the light response. Similar results were obtained when CaM kinases were blocked by KN-93. These findings place photoreceptor K^+ channels as an additional target for Ca^{2+}/calmodulin and suggest that I_K is well suited to act in concert with other components of the signaling machinery to sharpen light response termination and fine tune photoreceptor sensitivity during light adaptation.

Key words: potassium channels; phototransduction; calmodulin; light adaptation; photoreceptor; CaM kinase; Drosophila

Phototransduction in vertebrates and invertebrates is a complex signal transduction cascade, based on rhodopsin–G-protein coupling interactions (Hardie and Minke, 1995; Ranganathan et al., 1995; Baylor, 1996; Minke and Selinger, 1996; Zuker, 1996). The phototransduction process has the capacity to amplify single photon events into large electrical signals and to regulate the photoresponse output in a broad dynamic range. Major advances have been made in characterizing the molecular components of phototransduction and the mechanisms of light adaptation and response termination (Baylor, 1996; Minke and Selinger, 1996; Zuker, 1996). However, the modulation of these latter processes is not yet fully understood. The powerful combination of molecular genetics and electrophysiology makes *Drosophila* photoreceptors an exquisite preparation for studying these processes. In *Drosophila*, light activation of rhodopsin activates phospholipase C via G-proteins, which hydrolyzes phosphatidylinositol-4,5-bisphosphate into inositol trisphosphate (IP_3) and diacylglycerol (DAG). This process leads within a few tens of milliseconds to the opening of cation-selective channels encoded by the *trp* and *trp*-like genes (Hardie and Minke, 1995; Ranganathan et al., 1995; Minke and Selinger, 1996). The feedback control of the activation process was recently shown to involve calcium–calmodulin (Ca^{2+}/calmodulin), which tightly regulates the adaptation and termination of the light response (Arnon et al., 1997a,b; Scott and Zuker, 1997; Scott et al., 1997).

The photoreceptor potential has a complex waveform that arises from the opening of light-activated channels as well as from voltage-dependent conductances. Interestingly, *Drosophila* photoreceptors are endowed with high densities of voltage-gated K^+ channels (Hardie, 1991; Hardie et al., 1991). In neurons, K^+ channels were recognized to regulate action potential duration, firing patterns, and resting membrane potential (Rudy, 1988; Hille, 1992). A great diversity of K^+ channel subtypes appear to underlie these pleiotropic functions (Pongs, 1992; Doupnik et al., 1995; Salkoff and Jegla, 1995; Wickman and Clapham, 1995; Jan and Jan, 1997). Analysis of *Drosophila* mutants enabled the initial molecular characterization of several classes of K^+ channels (Kamb et al., 1987; Tempel et al., 1987; Pongs et al., 1988). Four different voltage-sensitive K^+ channel genes were initially identified in *Drosophila*: *Shaker* and *Shal*, encoding A-type K^+ currents (I_A), and *Shab* and *Shaw*, encoding delayed-rectifier K^+ currents (I_K) (Salkoff and Wymann, 1981; Wu and Haugland, 1985; Broadie and Bate, 1993; Tsunoda and Salkoff, 1995a,b). Subsequently, other classes of K^+ channels were characterized molecularly in *Drosophila* (Warmke et al., 1991; Goldstein et al., 1996; Titus et al., 1997; Wang et al., 1997).

Drosophila photoreceptors express both I_A and I_K currents, with the former mediated by subunits encoded by the *Shaker* locus (Hardie, 1991; Hardie et al., 1991). However, the genes encoding the delayed-rectifier channel subunits have not yet been

Received Aug. 5, 1998; accepted Aug. 26, 1998.

This research was supported by grants from the Israel Academy of Science, the Minerva Foundation, and the Dominic Einhorn Foundation (B.A). Dr. A. Peretz was supported by a Weizmann Institute postdoctoral fellowship (Koret fund) and by the Human Frontier Science Program. B.A. is an incumbent of the Philip Harris and Gerald Ronson Career Development chair. We thank Drs. Vivian Teichberg, Baruch Minke, and Eitan Reuveni for critical reading of this manuscript and helpful discussions. We are grateful to Emily Levine for careful reading of this manuscript. We also thank Wei-Dong Yao for communication of unpublished work.

Correspondence should be addressed to Dr. Bernard Attali, Department of Neurobiology, The Weizmann Institute of Science, Rehovot 76100, Israel.

identified, and very little is known about I_K modulation. Although the functional significance of I_A and I_K remains to be clarified in *Drosophila* phototransduction, in *Limulus* and in the blowfly *Calliphora vicina* they may regulate the gain and frequency response during light and dark adaptation (Fain and Lisman, 1981; Weckstrom et al., 1991). In *Drosophila* photoreceptors, the sustained depolarization generated by light activation of transient receptor potential (TRP) and transient receptor potential-like (TRPL) cationic channels is expected to open voltage-gated K^+ channels. One can predict that the subsequent hyperpolarizing K^+ currents will oppose the light-induced depolarizing currents to shape the photoreceptor potential.

In the present study, we show that *Drosophila* photoreceptor I_K and I_A channels are positively regulated by Ca^{2+}/calmodulin via a Ca^{2+}/calmodulin-dependent protein kinase (CaM kinase), with I_K being more sensitive than I_A. Using the current-clamp technique, we demonstrate that inhibition of I_K with K^+ channel blockers or with a CaM kinase inhibitor increases the amplitude and broadens the transient component of the photoreceptor potential, weakens adaptation, and slows the termination of the light response. We suggest that I_K represents an additional calmodulin-sensitive component of *Drosophila* phototransduction.

MATERIALS AND METHODS

Preparation. Wild-type (WT) *Drosophila* of the Canton S strain and of Sh^{KS133} mutant (both red-eyed) were used for the experiments (Wu and Ganetzky, 1992). The Sh^{KS133} allele, which eliminates the I_A, is a missense point mutation in the pore-forming H5 region of the *Shaker* channel protein (Lichtinghagen et al., 1990). Ommatidia dissociated from stage p15 pupae (Bainbridge and Bownes, 1981) were prepared as described previously (Hardie, 1991; Peretz et al., 1994). Retinae were rapidly dissected in Ca^{2+}/Mg^{2+}-free Ringer's solution, transferred to normal Ringer's solution supplemented with 10% fetal calf serum and 25 mM sucrose, and gently triturated with a fire-polished glass pipette of ~200–400 μm tip diameter. During the dissociation procedure, which requires no enzyme treatment, the surrounding pigment cells disintegrate, exposing the photoreceptor membrane. The dissection procedure was performed under dim red light illumination (Schott OG630 filter). Dark-adapted ommatidia were used immediately after dissection, for whole-cell patch-clamp recording.

Electrophysiology. Aliquots (~10 μl) of ommatidia were allowed to settle in a small chamber onto a clean coverslip mounted on the stage of an Axiovert 35 inverted microscope (Carl Zeiss). Recordings were made at 22 ± 1°C, using patch pipettes pulled from borosilicate glass capillaries (fiber filled) with resistance of 4–8 MΩ. Whole-cell recordings were performed using standard techniques (Hamill et al., 1981; Hardie, 1991; Peretz et al., 1994). In experiments investigating the light response, we applied the current-clamp mode of the whole-cell patch-clamp technique in isolated *Drosophila* photoreceptors. The resting potential of the photoreceptors was adjusted to −60 mV by applying a constant current. Series resistances were compensated by 85–90%. A tungsten halogen lamp (20 V, 150 W; Olympus Highlight 3000), attenuated by neutral density filters (1.5–2.0) via a Uniblitz shutter (Vincent Associates, Rochester, NY), provided illumination of photoreceptors. The peak transmission of the excitation and viewing filters was 520 and 630 nm, respectively. Signals were amplified using an Axopatch 200A patch-clamp amplifier (Axon Instruments, Foster City, CA), filtered below 2 kHz, via a four-pole Bessel filter. Data were sampled at 4–5 kHz and analyzed using pClamp 6.0.2 software (Axon Instruments) on an IBM-compatible 486 computer interfaced with DigiData 1200 (Axon Instruments). Further data analysis was performed using Axograph 3.0 software (Axon Instruments) and Excel 5.0 (MicroSoft) on an Apple Macintosh computer. All data were leakage-subtracted off line by the Clampfit program of the pClamp software. Activation and steady-state inactivation data were fitted with the Boltzmann distribution (assuming a reversal potential V_K of −85 mV):

$$I/I_{max} = a/\{1 + \exp[(V_{50} - V_K)/s]\}, \quad (1)$$

where V_{50} is the voltage of half-maximal activation (at which $I = 1/2\ I_{max}$), or the voltage at which half of the steady-state inactivation was removed, and s is the slope of the curve. In WT photoreceptors, I_A was measured at the peak, whereas I_K was measured at the end of the trace (~90 msec). All data were expressed as mean ± SEM. Statistically significant differences were assessed by Student's t test.

Solutions. Bath Ringer's solution contained 120 mM NaCl, 5 mM KCl, 1.5 mM CaCl, 8 mM $MgSO_4$, and 10 mM *N*-tris[hydroxymethyl]methyl-2-aminoethanesulfonic acid (TES), pH 7.15. Stock solutions of KN-62, KN-92, and KN-93 (Calbiochem, La Jolla, CA) were made in DMSO. *N*-(6 aminohexyl)-5-chloro-1-naphthalenesulfonamide (W7), trifluoperazine (TFP) TEA-Tetraethyfammonium, and quinidine (Sigma, St. Louis, MO) were added to the bath solution at the final concentrations indicated in text and figure legends. The pipette solution contained 135 mM potassium gluconate, 2 mM MgCl, 4 mM Mg-ATP, 0.5 mM Na-GTP, and 10 mM TES, pH 7.15.

RESULTS

Activation and inactivation characteristics of I_K and I_A in *Drosophila* photoreceptors

The whole-cell configuration of the patch-clamp technique (Hamill et al., 1981) was used to study the modulation of K^+ currents in dissociated *Drosophila* ommatidia. As shown in Figure 1, wild-type *Drosophila* photoreceptors are endowed with two main voltage-gated K^+ conductances, the rapidly activating/inactivating I_A and the slowly inactivating I_K currents (Hardie, 1991). The delayed-rectifier I_K current has previously been shown to be composed of two kinetically different components, I_{Kf} and I_{Ks} (Hardie, 1991). Using our activation protocol (Fig. 1), we were unable to discriminate accurately between these two I_K components, mainly because of the kinetic overlap of the various voltage-dependent rise times of activation. We could distinguish two different kinetic components of I_K in the mutant allele *Shaker KS133* (Sh^{KS133}) subjected to steady-state inactivation, when photoreceptor cells were treated with CaM kinase inhibitors (in five of eight cells; see below and Fig. 5). However, for the sake of clarity we have considered the delayed-rectifier K^+ current as one I_K component, distinguishable from the I_A current. Representative traces are shown in Figure 1*A* (*left*). Isolated I_K measurement was achieved by using the Sh^{KS133} mutation, which eliminates I_A (Fig. 1*B*, *left*). Sh^{KS133} is a missense point mutation in the H5 pore-forming region of the *Shaker* channel protein (Lichtinghagen et al., 1990). I_K was also measured in WT photoreceptors at the end of depolarizing pulses (~90 msec) after I_A has inactivated. The normalized current–voltage (*I–V*) relation of I_K as measured in WT or in Sh^{KS133} photoreceptors showed that I_K activated above −40 mV and saturated at potentials greater than +50 mV (Fig. 1*C*, *left*). In Sh^{KS133}, the normalized conductance during I_K activation was described by a single Boltzmann function with $V_{50} = +12.5 \pm 4.7$ mV, slope = -12.3 ± 0.9 mV ($n = 5$) (Fig. 2; see Table 2). A slight negative shift in the I_K current–voltage relation and normalized conductance curves measured in WT was seen when compared with those measured in Sh^{KS133} (Figs. 1*C*, 2*C,D*). This could result from incomplete inactivation of I_A in WT at the end of the depolarizing pulse, although a major part of I_A inactivated in our protocol. Alternatively, there could be a modulation of I_K activity attributable to developmental hyperexcitability of the Sh^{KS133} photoreceptors. Along this line, we found that I_K amplitude in Sh^{KS133} tends to be slightly higher than that measured in WT (Tables 1, 3). Such compensatory mechanisms are observed sometimes in transgenic knock-out mice.

As shown in the normalized *I–V* curve, I_A activated at potentials more negative than those required for I_K, above a threshold of approximately −60 mV (Fig. 1*D*, *left*). The normalized conductance of I_A activation was fitted with a single Boltzmann distribution of $V_{50} = -7.9 \pm 2.9$ mV and slope = -13.8 ± 0.3 mV

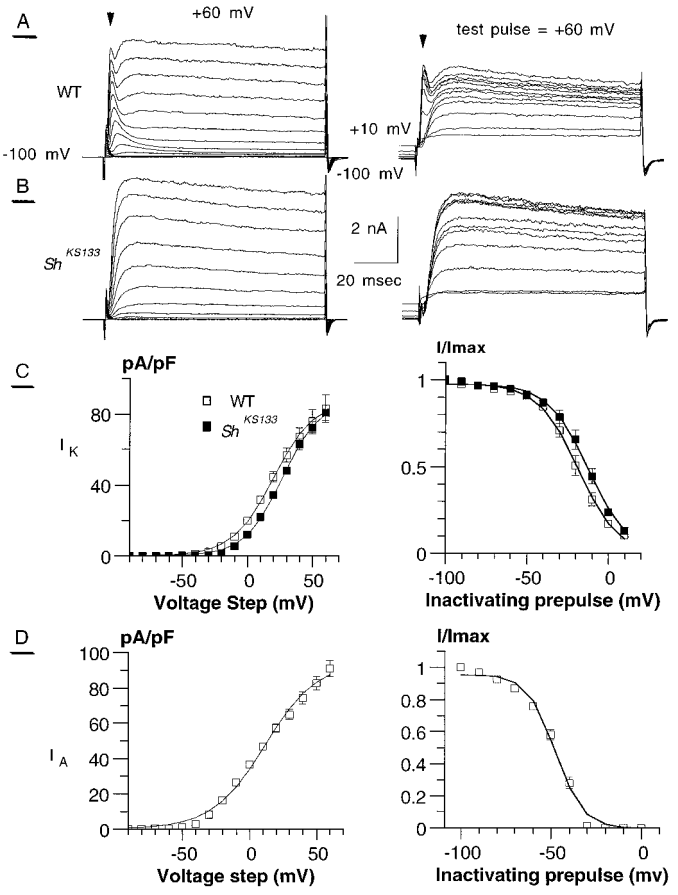

Figure 1. Activation and inactivation characteristics of I_A and I_K in *Drosophila* photoreceptors. *A*, Representative wild-type (*WT*) whole-cell recordings of photoreceptor potassium currents using the activation (*left*) and inactivation (*right*) protocols. Usually, we can clearly differentiate the inactivating I_A component (*arrowheads*) separated from the slowly inactivating I_K. *B*, Representative whole-cell recordings of activation (*left*) and inactivation (*right*) protocols of the *Shaker* mutant allele Sh^{KS133}. *C* (*left*), The current density (pA/pF) is plotted against the voltage steps for WT (□) and Sh^{KS133} (■). The I_K component is characterized (Boltzmann fitting, assuming a reversal potential $V_K = -85$ mV) by $I_{max} = 85.5 \pm 4.1$ pA/pF and 87.8 ± 5.6 pA/pF for WT ($n = 11$) and Sh^{KS133} ($n = 8$), respectively. *Right*, Steady-state inactivation of I_K in WT (□) and Sh^{KS133} (■). For Boltzmann fitting parameters, see Table 2. *D* (*left*), The current density/voltage curve of I_A is presented (Table 1). I_A is characterized (Boltzmann fitting, measured at peak outward current, assuming a reversal potential $V_K = -85$ mV) by $I_{max} = 92.3 \pm 7.8$ pA/pF ($n = 11$). *Right*, The Boltzmann fitting of I_A steady-state inactivation gave the values $V_{50} = -42.1 \pm 1.0$ mV and slope $= 10.0 \pm 0.8$ ($n = 4$). In all voltage-clamp experiments throughout this study, the holding potential was −100 mV. For the activation protocol, cells were stepped from −100 mV to +60 mV in 10 mV increments, during a 100 msec test pulse (*left column*). In the steady-state inactivation protocol, the cell membrane was subjected to inactivating prepulses of 1 sec duration from −90 mV to +10 mV in 10 mV increments, before 80 msec test pulse to +30 mV (*right column*).

($n = 5$) (Fig. 3; Table 2). Both currents inactivated in response to a depolarizing prepulse, with the I_A being inactivated at more hyperpolarized potentials. The steady-state inactivation of I_A and I_K could be described by a $V_{50} = -42.1 \pm 1.0$ mV, slope $= 10.0 \pm 0.8$ ($n = 4$), and $V_{50} = -18.9 \pm 2.1$ mV, slope $= 11.0 \pm 0.2$ ($n = 6$), respectively (Figs. 1*C,D, right*, 3, *right*; Table 2). The V_{50} values for I_A activation and steady-state inactivation of the present work are significantly shifted to more depolarized potentials (more than +10 mV) when compared with a recent study on a semi-intact retina preparation (Hevers and Hardie, 1995). Differences in recording conditions and solutions may account for these variations.

Ca^{2+}/calmodulin-dependent modulation of I_K

In view of the pivotal role played by Ca^{2+}/calmodulin in adaptation and termination of the light response (Arnon et al., 1997a,b; Scott et al., 1997), we tested whether photoreceptor I_A and I_K would be subjected to modulation by Ca^{2+}/calmodulin-dependent processes, and if so, to what extent it would affect the light response. To examine the possible Ca^{2+}/calmodulin-dependent modulation of I_K, we perfused the photoreceptor cells extracellularly with the calmodulin antagonist W7 at two different concentrations. Similar results were obtained using TFP, another calmodulin antagonist (data not shown). For all experiments, the currents were recorded on the same cell before and after application of the drug. Application of 2.5 μM W7 to WT photoreceptor cells led to a reduction of ~62% of the maximal I_K current density (I_{max}), whereas exposure of 25 μM W7 produced an almost complete inhibition of I_K (Fig. 2*A,C*; Table 1). The onset of W7 action was at ~1–2 min, and the effect reached steady state within ~5–7 min. Similar results were obtained when I_K was reordered in isolation in the Sh^{KS133} mutant, with 55% inhibition of I_K current density at 2.5 μM W7 and an almost complete I_K suppression on exposure to 25 μM W7 (Fig. 2*B,D*; Table 1). The normalized conductance of activation indicated that there was a small negative shift of V_{50} in the presence of 2.5 μM W7 (5.6 and 7 mV as measured in WT and Sh^{KS133}, respectively) (Fig. 2*C,D*; Table 2). Generally, the steady-state inactivation properties of I_K did not change significantly in response to 2.5 μM W7, as measured either in WT or in Sh^{KS133} mutant (Fig. 2*C,D*; Table 2).

Ca^{2+}/calmodulin regulation of I_A

Qualitatively, similar results were obtained for W7 action on I_A, except that the effects on I_{max} were much weaker. Furthermore, the effect of W7 on I_A might be slightly overestimated because of a minor contribution of the I_K rise. At 2.5 μM W7, current density at the peak of I_A was not significantly altered, with a decrease of <10% (Fig. 3; Table 1). At 25 μM W7, maximal I_A was substantially reduced (by 67%). The voltage dependence of activation and steady-state inactivation were significantly affected by W7. The V_{50} of I_A activation was negatively shifted from -7.9 ± 2.9 mV to $-19.8 \pm +1.7$ mV ($n = 5$) in response to 25 μM W7. In addition, there was a negative shift of the steady-state inactivation from $V_{50} = -42.1 \pm 1.0$ mV to $V_{50} = -48.8 \pm 2.5$ mV in response to 25 μM W7 ($n = 4$) (Fig. 3; Table 2).

A CaM kinase, identified as a calmodulin-dependent modulator of photoreceptor K^+ channels

The next question we asked was what type of calmodulin-dependent process was involved in the regulation of the photoreceptor K^+ currents. To examine this issue, we used the specific CaM Kinase inhibitors KN-93 (Sumi et al., 1991) and KN-62 (Tokumitsu et al., 1990). Only the data of KN-93 are presented here, because essentially the same results were obtained with KN-62 (data not shown). We focused on the I_K current because it proved to be more sensitive to W7. For this purpose, we used the Sh^{KS133} mutant to exclude any I_A contamination. Although I_K inactivated very little in the range of 100 msec (Fig. 1*B, left*), it underwent C-type inactivation (Hoshi et al., 1990) in a longer stimulation range (1 sec), and its inactivation could reach >50% (Figs. 4*D*, 5). We measured I_K amplitudes both at the peak and at the end of the pulse (plateau). After exposure to 5 μM KN-93, the

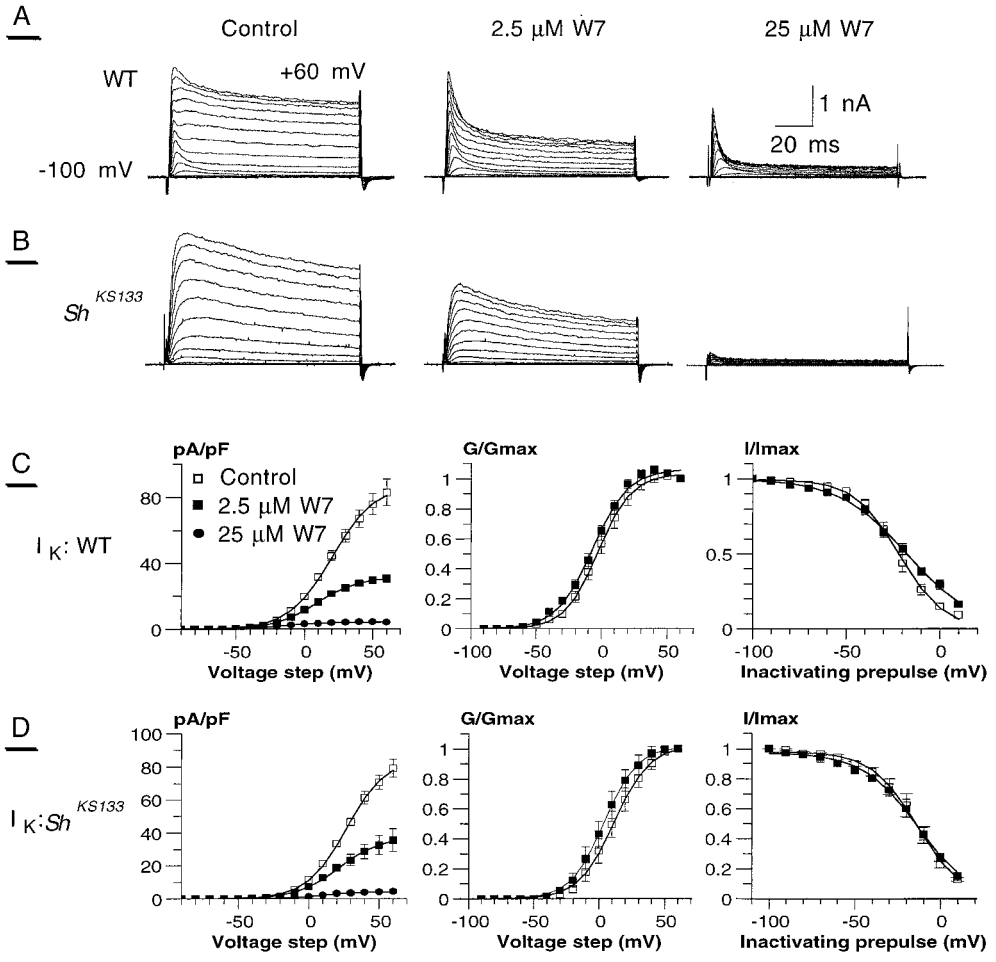

Figure 2. Inhibition of the delayed-rectifier current (I_K) by the calmodulin antagonist W7. The activation protocol as in Figure 1 is used to detect the steady-state effect of the calmodulin antagonist W7 on I_K currents. Traces were recorded 3–4 min after drug treatment. *A*, Whole-cell potassium currents, recorded in WT photoreceptors, were inhibited by W7 in a concentration-dependent manner. In response to 2.5 μM W7, I_K was reduced by >50% (*middle*), whereas 25 μM W7 almost completely abolished the current (*right*), as compared with control (*left*). *B*, Similar results were obtained in the Sh^{KS133} mutant, which lacks the I_A. *C, D*, The current density/voltage curve for WT (*C, left*) and Sh^{KS133} (*D, left*) and their corresponding normalized conductance (*C, D, middle*) are shown for control (□), 2.5 μM W7 (■), and 25 μM W7 (●) data. The steady-state inactivation protocol was the same as in Figure 1 (*right*; traces not shown). Because of almost complete inhibition of I_K, no steady-state inactivation curves could be determined after treatment with 25 μM W7. The curves were fitted by the Boltzmann distribution function. For fitting values see Tables 1 and 2.

Table 1. W7 effect on the I_{max} in WT and Sh^{KS133}

	I_{max} (pA/pF)		
	Control	2.5 μM W7	25 μM W7
I_K: WT	82.5 ± 4.1 (11)	31.6 ± 2.6 (5)*	4.2 ± 0.4 (6)*
I_K: Sh^{KS133}	87.8 ± 5.6 (9)	39.2 ± 8.9 (5)*	4.4 ± 1.0 (4)*
I_A: WT	92.3 ± 7.8 (11)	85.1 ± 11.3 (6)	30.1 ± 2.8 (6)*

The maximal current density I_{max} (pA/pF) was obtained from the fit of a single Boltzman distribution (see Eq. 1; assuming a reversal potential of −85 mV for both I_A and I_K) on the normalized current–voltage relations determined for WT and Sh^{KS133} in the absence and presence of W7. The data are presented as mean ± SEM, with the number of cells in parentheses. Except for the action of 2.5 μM W7 on I_A, all of the W7 effects were statistically significant (*$p < 0.01$, Student's t test).

amplitudes of the peak and plateau components of I_K were reduced by 62% (from 107.1 ± 6.8 pA/pF to 40.7 ± 6.1 pA/pF) and 85% (from 65.7 ± 6.3 pA/pF to 10.1 ± 1.2 pA/pF), respectively ($n = 6$) (Fig. 4*A,D, top traces*; Table 3). The effect of KN-93 was very specific because the application of its structurally related but functionally inactive analog KN-92 (5 μM) did not produce any effect on I_K even after longer exposure (>15 min) (Fig. 4*D*). Furthermore, to exclude the possibility that KN-93 could act as an open-channel blocker, we used a train protocol. KN-93 inhibition was obtained at the first pulse (+60 mV) after a 5 min exposure to the drug, and the effect did not significantly increase further after subsequent stimulations. The onset of KN-93 inhibitory action was at ~2 min after application, and it peaked at ~5–6 min. Because KN-93 was delivered along with the carrier DMSO at a final concentration of 0.1%, we checked for possible effects of the solvent carrier. We found that DMSO alone affected neither I_K nor the light response (data not shown). KN-93 caused a significant change in the voltage dependence of activation. The normalized conductance curves indicated a negative shift of the V_{50} by 11.5 and 8.7 mV for the peak and plateau components, respectively (Fig. 4*B*; Table 3). KN-93 also caused the I_K to inactivate at more negative potentials. The V_{50} of steady-state inactivation was shifted from −12.7 ± 0.6 mV to −22.3 ± 2.4 mV ($n = 6$) (Fig. 4*C*; Table 3), an effect not seen in response to W7 treatment (see Discussion).

CaM kinase inhibition accelerated I_K inactivation kinetics

It is known that K^+ channels exhibit two different mechanisms of inactivation, referred to as N- and C-type inactivations (Hoshi et al., 1990; Choi et al., 1991; Yellen et al., 1994). Although N-type inactivation is a fast process involving the occlusion of the inner mouth of the channel pore by the amino terminus (ball and chain model), C-type inactivation is a slower process occurring after prolonged depolarization and involving conformational changes at the external mouth of the pore and the S6 transmembrane domain. As shown in Figure 5, after step depolarization of 1 sec duration from −100 mV to +60 mV, I_K underwent a slow C-type inactivation process by >50%. In Figure 5*A,B*, the traces have been normalized to compare the kinetics. After 6 min of 5 μM KN-93 application on Sh^{KS133} photoreceptor cells, I_K decreased in amplitude and inactivated with faster kinetics when compared

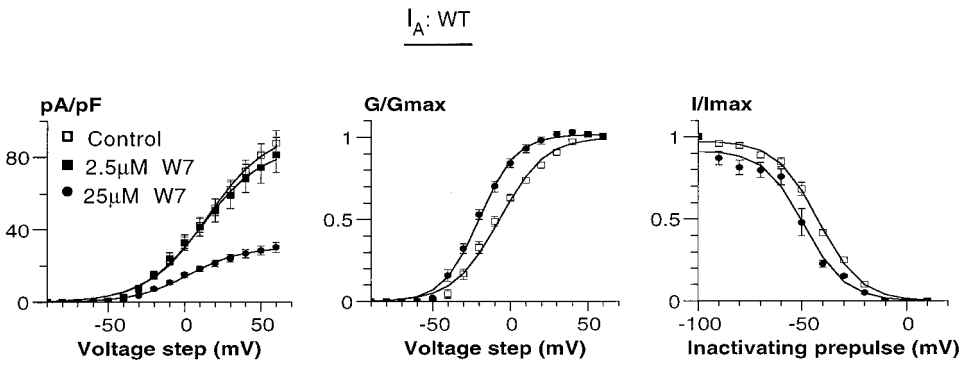

Figure 3. The effect of W7 on I_A. The current density/voltage curve (*left*), their normalized conductance (*middle*), and the corresponding steady-state inactivation curves (*right*) are shown for control (□), 2.5 μM W7 (■), and 25 μM W7 (●) data. Because little effect on I_A was observed in the presence of 2.5 μM W7, only the data obtained with 25 μM W7 were included in the normalized conductance and steady-state inactivation curves. All of the curves were fitted by Boltzmann distributions. For details of the fitting values, see Tables 1 and 2.

Table 2. Effect of W7 on the steady-state activation and inactivation parameters in WT and *Sh*^{KS133}

		V_{50} (mV)		Slope (mV/e-fold)	
		Control	Drug	Control	Drug
Activation					
2.5 μM W7	I_K: WT (5)	−1.5 ± 4.4	−7.1 ± 2.4	−12.4 ± 0.6	−13.4 ± 0.6
	I_K: *Sh*^{KS133} (5)	12.5 ± 4.7	5.5 ± 5.2	−12.3 ± 0.9	−11.8 ± −1.1
25 μM W7	I_A: WT (5)	−7.9 ± 2.9	−19.8 ± 1.7*	−13.8 ± 0.3	−11.5 ± 0.4
Inactivation					
2.5 μM W7	I_K: WT (6)	−18.9 ± 2.1	−18.0 ± 2.7	11.0 ± 0.2	17.5 ± 1.0
	I_K: *Sh*^{KS133} (4)	−14.3 ± 4.1	−14.2 ± 3.1	11.8 ± 0.8	16.1 ± 1.9
25 μM W7	I_A: WT (4)	−42.1 ± 1.0	−48.8 ± 2.5	10.0 ± 0.8	9.8 ± 0.6

The activation and inactivation parameters determined in the absence or presence of W7 were fitted by a single Boltzman distribution (see Eq. 1) and summarized by V_{50} (mV) and by the slope (mV/e-fold) of the voltage dependence. The normalized conductance was calculated using the Ohm's law assuming a K^+ reversal potential of −85 mV, for both I_A and I_K. The data are presented as mean ± SEM, with the number of cells in parentheses. *$p < 0.05$, Student's *t* test.

with control (Fig. 5*A*). Similar results were obtained with 10 μM W7 application (Fig. 5*B*). After a 5 min W7 washout, there was a partial recovery in terms of both amplitude and kinetics. Note that neither the deactivation kinetics [as reflected by the tail current decay (Fig. 5*A, inset*)] nor the rising phase of current activation was changed in the presence of W7 or KN-93 (Fig. 5*A, right*). I_K inactivation kinetics was best fitted with two exponentials. In response to 5 μM KN-93, the decay time constants were significantly reduced from $\tau_1 = 86 \pm 10$ msec and $\tau_2 = 767 \pm 29$ msec to $\tau_1 = 30 \pm 3$ msec and $\tau_2 = 514 \pm 34$ msec ($n = 6$, $p < 0.005$). Regarding the activation kinetics, we have considered the photoreceptor I_K to be one component. As mentioned earlier, it was suggested by Hardie (1991) that the *Drosophila* delayed-rectifier currents are composed of two conductances, I_{Kf} and I_{Ks}, with fast and slow activation kinetic components. Results consistent with this suggestion were obtained in KN-93-treated *Sh*^{KS133} photoreceptors by using a steady-state inactivation protocol (Fig. 5*C*). In the control traces, it was difficult to discriminate between the two kinetic components (Fig. 5*C, left*). However, when photoreceptor cells (in four of seven cells) were exposed to 5 μM KN-93 for 6 min (Fig. 5*C, right*), it became obvious that a fast component was more sensitive to inactivating prepulse potentials, as compared with a slower activating component that inactivated more weakly at the same prepulses. Similar results were obtained with W7 in seven of eight cells recorded. Nevertheless, it was difficult to distinguish between these two components when fitting the steady-state inactivation curve (Fig. 4*C*). Thus, it is possible that inhibition of CaM kinase affects differently the two kinetic components of C-type inactivation, thereby reflecting the existence of two different I_K conductances. However, we cannot exclude the possibility that these kinetic components represent different conformational kinetic transitions of the same channel complex.

Inhibition of I_K reduced the light adaptation and delayed the response termination

To test whether photoreceptor K^+ currents oppose the light-induced depolarizing currents and shape the light response, we investigated their role in phototransduction by pharmacological means using the current-clamp technique in isolated photoreceptors of the WT and the *Drosophila* mutant *Sh*^{KS133}, which eliminates I_A. To quantitatively estimate the drug effects on photoreceptor potential waveform, we used the quotient Q_{50} defined as a ratio value ($Q_{50} = T_D/T_C$) of the measurements made in the presence (T_D) and absence (T_C) of the drug. T_D and T_C are temporal parameters (in milliseconds) measuring the width of the light response at 50% of the maximal receptor potential amplitude evoked by illumination. First, we studied in WT photoreceptors the voltage light response before and after CaM kinase inhibition by application of 5 μM KN-93 (Fig. 6*A*). After a 10 msec flash stimulus, KN-93 (6 min preincubation) significantly increased the light response amplitude and markedly delayed its termination, as compared with control with a $Q_{50} = 1.84 \pm 0.15$ ($p < 0.05$, $n = 4$) (Fig. 6*A, left*). To evaluate the effects of KN-93 on the light adaptation process, a 500 msec light stimulus was given before and after application of the drug. As shown in Figure 6*A* (*right*), KN-93 not only increased the amplitude of the receptor potential but also broadened the transient component of the light response and weakened the dip between the peak and the plateau ($Q_{50} = 1.99 \pm 0.17$, $n = 4$, $p < 0.05$). To focus on the K^+ channel contribution, we investigated the effects of two different K^+ channel blockers, TEA and quinidine (Fig. 6*B*). After a 10

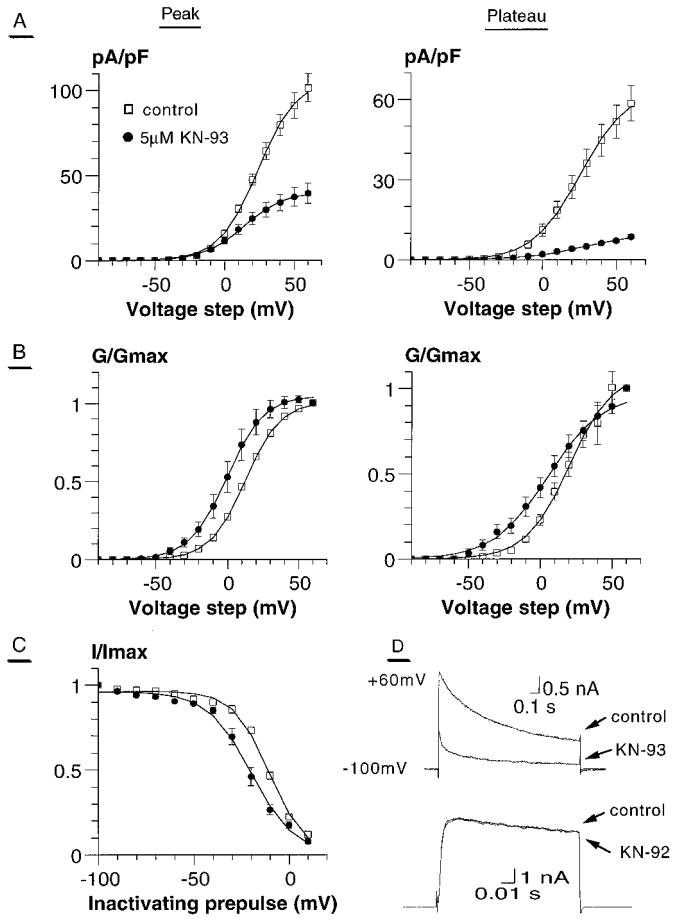

Figure 4. Modulation of I_K by the CaM kinase inhibitor KN-93 in the Sh^{KS133} mutant. The specific CaM kinase inhibitor KN-93 modulates the peak and plateau components of I_K in the Sh^{KS133} mutant. In the experiments, the currents were recorded on the same cell before and after 6 min application of the drug. Except for *C*, the cells were stepped from −100 to +60 mV in 10 mV increments, and the peak and plateau currents were measured during the 1 sec pulse. The curves were fitted by a single Boltzmann distribution. Results were obtained from six pupae. *A*, The current density/voltage curve is shown for control (□) and in response to 5 μM KN-93 (■) at the peak (*left*) and plateau (*right*) of I_K. *B*, The normalized conductance curves are shown for the peak (*left*) and plateau component (*right*) of I_K. The same symbols were used as in *A*. For the fitting values, see Table 3. *C*, The steady-state inactivation curve of I_K is shown. Here the inactivation protocol was the same as in Figure 1. For detailed Boltzmann fitting values see Table 3. *D* (*top traces*), Representative example of the KN-93 (5 μM) effect on I_K. From a holding potential of −100 mV, a step to +60 mV (1 sec) was given before and after (9 min) drug application. *Bottom traces*, Cell stepped from a holding potential of −100 to +60 mV (100 msec) before and 10 min after KN-92 treatment (5 μM).

msec flash stimulus, there was an enhancement of the receptor potential amplitude and a marked slowing of light response termination in the presence of the general K^+ channel blocker TEA (20 mM) ($Q_{50} = 1.76 \pm 0.36, n = 6, p < 0.05$). Similar results were obtained with 0.2 mM quinidine, previously shown to block delayed-rectifier K^+ channels in *Drosophila* (Singh and Wu, 1989), with a $Q_{50} = 2.12 \pm 0.17$ ($n = 4, p < 0.05$). After a 500 msec light stimulus, quinidine (0.2 mM) strongly inhibited the light adaptation process with a much broader transient and an almost complete elimination of the plateau ($Q_{50} = 2.21 \pm 0.33$, $n = 5, p < 0.01$) (Fig. 6*B, right*). Figure 6*C* illustrates to what extent quinidine (0.2 mM) preferentially blocked I_K currents in WT photoreceptors (compare with Sh^{KS133} in Fig. 7*C*). However, we noticed that at this concentration (0.2 mM), quinidine also reduced by ~20% the I_A currents in WT cells (Fig. 6*C*).

To evaluate the contribution of I_A in light response adaptation and termination, we performed the same experiments in Sh^{KS133} photoreceptor cells (Fig. 7). The photoreceptor potential waveform was very similar in Sh^{KS133} mutants as compared with WT photoreceptors after either a 10 msec flash or a 500 msec light stimulus (Figs. 6, 7*A,B*). The Sh^{KS133} mutation affected neither the light adaptation nor the voltage waveform, including the transient, the dip, and the plateau phases (Fig. 7*A*). As compared with WT cells, essentially the same effects of TEA and quinidine were obtained in Sh^{KS133} photoreceptors, with an increased amplitude and a broadening of the photoreceptor potential as well as a slowing down of the turn-off responses to flash stimuli (Fig. 7*B*). After a 10 msec flash, the Q_{50} of TEA (20 mM) and quinidine (0.2 mM) was 1.41 ± 0.04 ($n = 5, p < 0.001$) and 2.00 ± 0.26 ($n = 4$, $p < 0.05$), respectively. Similar results were obtained with KN-93 (data not shown). Figure 7*C* shows that quinidine (0.2 mM) blocked virtually all I_K currents in Sh^{KS133} photoreceptors.

Finally, we investigated the possible modulation of I_K by light. We compared I_K in dark-adapted cells and during a 10–100 msec flash stimulus that generates an approximately +10 mV depolarization. I_K was measured under voltage-clamp by stepping cells for 100 msec from −80 mV to −10 mV. After subtracting the light-induced current, we found no significant effects on I_K kinetics or amplitude (<10%) (data not shown).

DISCUSSION

For what functional purpose are *Drosophila* photoreceptors endowed with high densities of voltage-gated K^+ channels (Hardie, 1991; Hevers and Hardie, 1995)? Given their magnitude, voltage operating range, and kinetics, it was crucial to elucidate whether these K^+ conductances are subject to modulation and to evaluate their functional significance in phototransduction. The present work shows that *Drosophila* photoreceptor K^+ channels are modulated by a CaM kinase, and as such may act in concert with other calmodulin-sensitive components to play a role in the feedback control of the light response.

Drosophila photoreceptor neurons have evolved an exquisitely sophisticated signaling machinery to turn on the light response. This leads to the opening of TRP and TRPL cationic channels and generates a depolarizing receptor potential (Ranganathan et al., 1995; Minke and Selinger, 1996; Zuker, 1996) that is expected to activate the voltage-gated K^+ channels. On light stimulation, photoreceptor cells are likely to operate within potentials ranging from approximately −60 mV to +10 mV. Considering the voltage operating range values we found for I_A and I_K (Figs. 1, 3; Table 2), it is reasonable to assume that these K^+ conductances will be operative within the voltage limits of photoreceptor activity.

Our data show that photoreceptors I_K and I_A are specifically inhibited by different Ca^{2+}/calmodulin antagonists such as W7 or TFP, with I_K being far more sensitive than I_A. Interestingly, this modulation was mimicked by two selective CaM kinase antagonists, KN-62 and KN-93. The inability of KN-92 (inactive structural analog of KN-93) to affect I_K demonstrates the specificity of KN-93 action. The mechanisms whereby I_K and I_A are depressed after exposure to CaM kinase inhibitors are not elucidated yet, but may involve either a direct channel phosphorylation or an indirect modulation. With respect to indirect regulation, it is possible that the CaM kinase mediates its effect via the *eag* channel subunit, as suggested previously (Zhong and Wu, 1993).

Table 3. Effect of KN-93 on I_{max}, normalized conductance and steady-state inactivation of I_K in Sh^{KS133}

	Current	G/G_{max}		Inactivation	
	I_{max} (pA/pF)	V_{50} (mV)	Slope (mV/e-fold)	V_{50} (mV)	Slope (mV/e-fold)
Peak (6)					
Control	107.1 ± 6.8	12.7 ± 0.9	−12.4 ± 0.3	−12.7 ± 0.6	10.7 ± 0.6
5 μM KN-93	40.7 ± 6.1**	1.2 ± 4.8*	−11.6 ± 1.1	−22.3 ± 2.4**	10.3 ± 0.7
Plateau (6)					
Control	65.7 ± 6.3	24.0 ± 1.0	−15.5 ± 0.6	−10.4 ± 0.6	9.3 ± 0.3
5 μM KN-93	10.1 ± 1.2**	15.3 ± 9.9	−20.4 ± 1.7	−19.6 ± 2.2**	10.5 ± 0.3

The maximal current amplitude I_{max} was obtained from the fit of a single Boltzman distribution (see Eq. 1) on the normalized (pA/pF) current–voltage relations and measured in Sh^{KS133} in the absence and presence of 5 μM KN-93. The activation and inactivation parameters determined in the absence or presence of 5 μM KN-93 were analyzed as in Table 2. The data are presented as mean ± SEM, with the number of cells in parentheses. $^*p < 0.05$, $^{**}p < 0.001$, Student's *t* test.

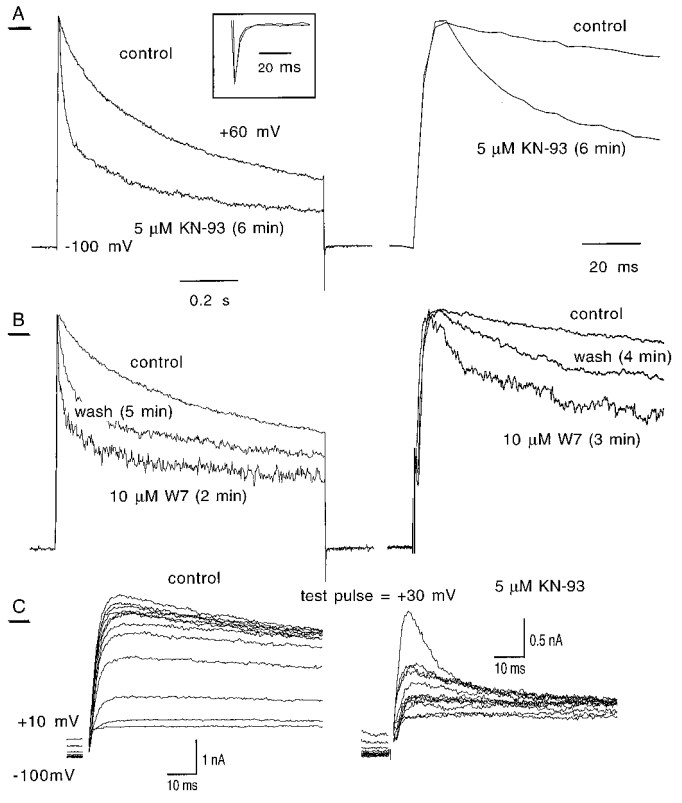

Figure 5. Changes in I_K kinetics in response to W7 and KN-93. Using the Sh^{KS133} mutant, photoreceptor cells were stepped from −100 to +60 mV for 1 sec to allow the C-type inactivation of I_K to occur. *A* (*left*), The currents were recorded before (*control*) and after 6 min application of 5 μM KN-93. Traces have been normalized for kinetic comparison. *Right*, The same normalized traces are shown at a smaller time scale. *Inset*, The normalized tail currents are shown. The C-type inactivation kinetics are well described by two exponential fits. In response to 5 μM KN-93, the fast and slow time constants (τ1 and τ2) decreased from 86 ± 10 to 30 ± 03 msec and from 767 ± 29 to 514 ± 34 msec, respectively ($n = 6, p < 0.01$). *B* (*left*), Similar results were obtained in response to 2 min exposure of 10 μM W7, with a partial recovery 5 min after washout of the drug. *Right*, Another experiment demonstrates the same phenomena at a smaller time scale and higher sampling rate. *C*, Steady-state inactivation traces, before and 5 min after application of 5 μM KN-93. The same steady-state inactivation protocol was used as in Figure 1.

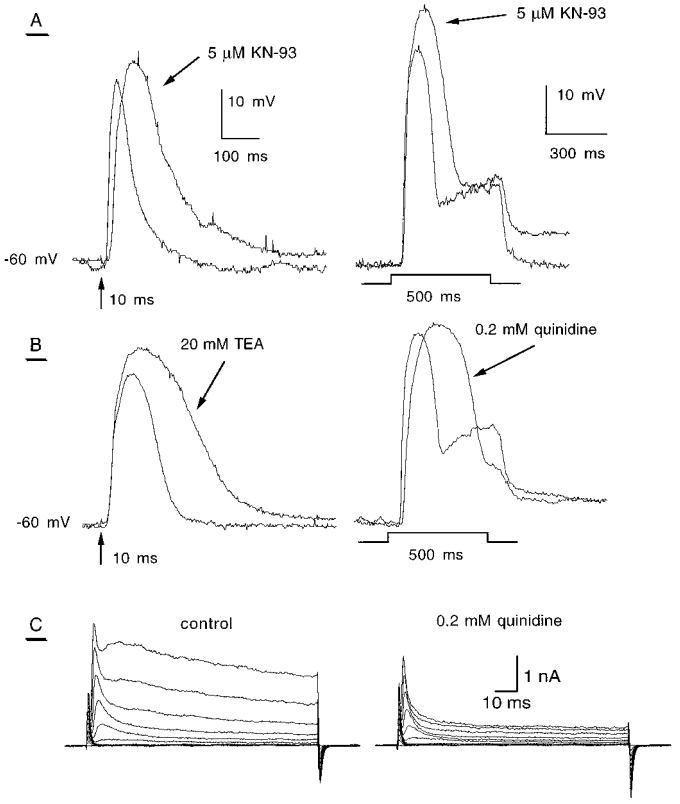

Figure 6. Effect of K^+ channel blockers and a CaM kinase antagonist on the light response of WT photoreceptors. *A, B*, Whole-cell current-clamp recordings of the light response were performed in WT photoreceptors. In the current-clamp mode the resting potential was adjusted to −60 mV. The resting potential before adjustment ranged between −35 and −45 mV. *Left*, A light flash (10 msec, *arrow*) was given to dark-adapted photoreceptors (>2 min), and the light response was recorded before and 4 min after exposure of 5 μM KN-93 or 3 min after application of 20 mM TEA. Traces shown are representative of four similar experiments. *Right*, The same procedure was used except the light stimulus duration was 500 msec. Effects of the I_K channel blocker quinidine (0.2 mM, five experiments) and of the CaM kinase inhibitor KN-93 (5 μM, five experiments) are shown in representative traces. *C*, Whole-cell voltage-clamp recordings of cells before (*control, left*) and 2 min after application of 0.2 mM quinidine (*right*). The activation protocol was the same as in Figure 1.

A striking consequence of CaM kinase inhibition was the accelerated C-type inactivation kinetics of I_K as revealed by exposure of Sh^{KS133} photoreceptors to KN-93 or W7. Blockade of CaM kinase-mediated phosphorylation may alter the local charge distribution in a specific channel domain, thereby affecting directly or allosterically the kinetics of C-type inactivation, through long-range electrostatic interactions. A very similar modulation by CaM kinase has been reported recently for Kv1.4 K^+ channels (Roeper et al., 1997). Blockade of CaM Kinase II by KN-93 was found to accelerate the Kv1.4 inactivation rate constants by 5- to

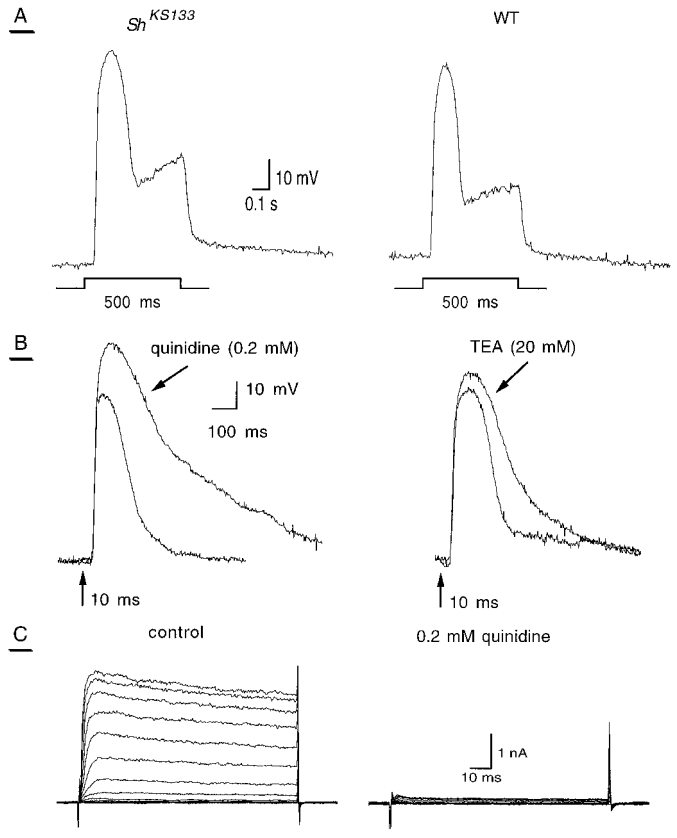

Figure 7. Effect of K^+ channel blockers on the light response of Sh^{KS133} photoreceptors. *A, B*, Whole-cell current-clamp recordings of the light response were performed in Sh^{KS133} photoreceptors. *A*, Voltage responses to light stimuli (500 msec) recorded in WT (*right*; representative of seven cells) and Sh^{KS133} (*left*; representative of six cells) photoreceptors. *B*, Voltage responses of Sh^{KS133} photoreceptors to a 10 msec flash in the absence and presence of 0.2 mM quinidine (*left*; representative of five cells) and 20 mM TEA (*right*; representative of four cells). *C*, Whole-cell voltage-clamp recordings of Sh^{KS133} photoreceptors before (*control, left*) and 2 min after application of 0.2 mM quinidine (*right*). The activation protocol was the same as in Figure 1.

10-fold, suggesting that CaM kinase phosphorylation is likely to affect the interplay between N- and C-type inactivation (Roeper et al., 1997). The origin of the shift toward negative potentials (~10 mV) in steady-state activation of I_K and I_A evoked by KN-93 and W7, respectively, is unclear. However, blockade of CaM kinase-mediated phosphorylation may alter the net charge in the vicinity of the channel voltage sensor and thus affect the voltage-dependent gating (Perozo and Bezanilla, 1990). It is worth noting that W7 did not produce a substantial leftward shift in the steady-state activation and inactivation curves of I_K (Fig. 2), suggesting that the Ca^{2+}/calmodulin effects may not be mediated solely by a CaM kinase.

Our results indicate that I_K is more sensitive than I_A to modulation by a CaM kinase in photoreceptor cells. A similar higher sensitivity of I_K as compared with I_A with regard to CaM kinase modulation was recently found in cultured *Drosophila* neurons (W.-D. Yao and C.-F. Wu, personal communication). The channel subunit gating the I_A current in *Drosophila* photoreceptors was found to be encoded by the *Shaker* locus (Hardie et al., 1991). Although the native oligomeric structure of I_A is not known, Hardie et al. (1991) suggested previously that it is encoded by some of the *Shaker* isoforms, possibly *Sh*A1, *Sh*A2, *Sh*G1, or *Sh*G2. The situation is even more complex for the identity of I_K. We found by PCR that *Shab* 1 and *Shab* 2 isoforms as well as *Shaw* transcripts are expressed in *Drosophila* retina (our unpublished data), indicating that *Shab* and *Shaw* gene products could possibly be direct or indirect substrates of CaM kinase regulation. In this regard, it is worth noting that the *Shab* channel subunit contains four consensus sites for phosphorylation by CaM kinase [XRXXS (Pearson and Kemp, 1991)] at its intracellular amino and C termini.

Ca^{2+}/calmodulin is known to regulate various downstream targets, including CaM kinase as well as additional components involved in phototransduction (Arnon et al., 1997a,b; Scott et al., 1997). Modulation of I_K mediated by CaM kinase thus represents one of the effects of Ca^{2+}/calmodulin on receptor potential. Considering that photoreceptor cells were recorded in the dark, our data imply that in resting dark-adapted conditions there is a marked basal phosphorylation of K^+ channels by CaM kinase. Resting cytoplasmic free Ca^{2+} levels in the dark (in the presence of 1.5 mM external Ca^{2+}) range within 130 and 180 nM (Hardie, 1996). These values are apparently sufficient to elicit substantial CaM kinase activity in the dark (Friedman et al., 1986; Braun and Schulman, 1995; Soderling, 1996). Within the operating window of the photoreceptor potential (−60 mV to +10 mV), the activation of I_K and I_A is still far from saturation, leaving many K^+ channels to be recruited by increased CaM kinase activity after light stimulation. However, we could not detect a significant upregulation of I_K by light. This result does not exclude a role for CaM kinases in regulating I_K activity during light stimulation. Indeed, under our experimental conditions light stimulation could also activate Ca^{2+}/calmodulin-dependent phosphatases (e.g., calcineurin), which may tightly interact with the channel complex leaving a steady-state phosphorylation almost unchanged. Thus, I_K channel activity may be accounted for by a fine tuning of Ca^{2+}/calmodulin-dependent kinases and phosphatases. Interestingly, a recent report described the existence of a signaling complex consisting of the stable association of the protein phosphatase PP2A with CaM kinase IV (Westphal et al., 1998). PP2A dephosphorylates CaM kinase IV and functions as a negative regulator of CaM kinase IV signaling (Westphal et al., 1998).

From a functional point of view, our current-clamp data show for the first time in *Drosophila* that voltage-gated K^+ channels play a significant role in adaptation and termination of the light response. Similar observations were reported in photoreceptors of the blowfly *C. vicina* (Weckstrom et al., 1991), in which K^+ channels were suggested to reduce the membrane time constant, thus enabling the photoreceptors to code high frequencies in light-adapted cells. Previous work performed in *Limulus* suggested that the dip between the transient and the plateau phase of the photoreceptor potential could be accounted for by the I_A channel activity (O'Day et al., 1982). This dip was consistently observed in the voltage light response recorded from Sh^{KS133} photoreceptors (Fig. 7*A*), excluding a significant contribution of I_A to this phase of the receptor potential waveform. Furthermore, inhibition of CaM kinase by KN-93 or blockade of I_K channels by quinidine and TEA reproduced the same effects on either Sh^{KS133} mutant or WT photoreceptors. Although we did not notice major differences in the potential waveforms between WT and Sh^{KS133} mutants, we cannot totally exclude a possible role of I_A in the light response. Clearly, the decreased light adaptation and the slowing down of the turn-off kinetics produced by TEA and quinidine point to I_K as the main K^+ conductance involved in the regulation of the light response. It is worth noting that KN-93

broadened the transient component of the light response but did not reduce the plateau phase as elicited by K^+ channel blockers. A likely explanation is that 5 μM KN-93 did not completely abolish I_K (Fig. 4; Table 3), whereas 0.2 mM quinidine almost totally suppressed I_K in Sh^{KS133} photoreceptors (Fig. 7).

The gating mechanisms of light-activated channels remain a matter of controversy. It has been proposed that calcium release from internal stores is required for activation of phototransduction and that the TRP channel functions as a store-operated channel. In this view, TRP is gated by the depletion of internal stores (Minke and Selinger, 1996; Arnon et al., 1997a,b). However, recent studies challenged this hypothesis and suggest that IP_3 receptors and internal stores are not required for the activation of the light response (Scott et al., 1997). However, Ca^{2+}/calmodulin was recently found to tightly control the light response by modulating the various components previously established in the *Drosophila* phototransduction process. Ca^{2+}/calmodulin was shown to mediate light adaptation through its negative feedback on IP_3- and ryanodine-sensitive stores, thereby dampening the Ca^{2+}-induced Ca^{2+} release amplification process (Arnon et al., 1997a,b). Likewise, Ca^{2+}/calmodulin was found to control termination of the light response via its inhibitory action on TRPL channels and its positive regulation of arrestin activity (Scott et al., 1997). For example, arrestin I (also called phosrestin I in photoreceptors) undergoes light-induced phosphorylation on a subsecond time scale, via CaM kinase II activity (Matsumoto et al., 1994; Kahn and Matsumoto, 1997). A recent study in *Limulus* photoreceptors showed that Ca^{2+}/calmodulin could even exert its control via inhibition of phospholipase C, and this may also apply to the *Drosophila* phototransduction process (Richard et al., 1997). The modulation of I_K by CaM kinase supports the notion that K^+ channels represent an additional calmodulin-sensitive component of the negative feedback control of the light response. We suggest that I_K acts in concert with other Ca^{2+}/calmodulin-sensitive elements of the transduction cascade to regulate the gain, to control the waveform of the light-activated receptor potential, and to extend the operating range of photoreceptors.

REFERENCES

Arnon A, Cook B, Montell C, Selinger Z, Minke B (1997a) Calmodulin regulation of calcium stores in phototransduction of *Drosophila*. Science 275:1119–1121.

Arnon A, Cook B, Gilo B, Montell C, Selinger Z, Minke B (1997b) Calmodulin regulation of light adaptation and stored-operated dark current in *Drosophila* photoreceptors. Proc Natl Acad Sci USA 94:5894–5899.

Bainbridge SP, Bownes M (1981) Staging the metamorphosis of *Drosophila melanogaster*. J Embryol Exp Morphol 66:57–80.

Baylor D (1996) How photons start vision. Proc Natl Acad Sci USA 93:560–565.

Braun AP, Schulman H (1995) The multifunctional calcium/calmodulin dependent protein kinase: from form to function. Annu Rev Physiol 57:417–445.

Broadie KS, Bate M (1993) Development of larval muscle properties in the embryonic myotubes of *Drosophila melanogaster*. J Neurosci 13:167–180.

Choi KL, Aldrich RW, Yellen G (1991) Tetraethylammonium blockade distinguishes two inactivating mechanisms in voltage-activated K^+ channels. Proc Nat Acad Sci USA 88:5092–5095.

Doupnik CA, Davidson N, Lester HA (1995) The inward rectifier potassium channel family. Curr Opin Neurobiol 5:268–277.

Fain GL, Lisman JE (1981) Membrane conductances of photoreceptors. Prog Biophys Mol Biol 37:91–147.

Friedman Y, Henricks L, Poleck T, Levasseur S, Burke G (1986) Calcium-activated, calmodulin-dependent protein kinase activity in bovine thyroid cytosol. Biochem Biophys Res Commun 140:120–127.

Goldstein SA, Price LA, Rosenthal DN, Pausch MH (1996) ORK1, a potassium-selective leak channel with two pore domains cloned from *Drosophila* melanogaster by expression in *Saccharomyces cerevisiae*. Proc Natl Acad Sci USA 93:13256–13261.

Hamill OP, Marty A, Neher E, Sakmann B, Sigworth FJ (1981) Improved patch-clamp techniques for high resolution current recording from cells and cell free membrane patches. Pflügers Arch 391:85–100.

Hardie RC (1991) Voltage-sensitive potassium channels in *Drosophila* photoreceptors. J Neurosci 11:3079–3095.

Hardie RC (1996) INDO-1 measurements of absolute resting and light-induced Ca^{2+} concentration in *Drosophila* photoreceptors. J Neurosci 16:2924–2933.

Hardie RC, Minke B (1995) Phosphoinositide-mediated phototransduction in *Drosophila* photoreceptors: the role of Ca^{2+} and *trp*. Cell Calcium 18:256–274.

Hardie RC, Voss D, Pongs O, Laughlin SB (1991) Novel potassium channels encoded by the *Shaker* locus in *Drosophila* photoreceptors. Neuron 6:477–486.

Hevers W, Hardie RC (1995) Serotonin modulates the voltage dependence of delayed rectifier and *Shaker* potassium channels in *Drosophila* photoreceptors. Neuron 14:845–856.

Hille B (1992) Ionic channels of excitable membranes. Sunderland, MA: Sinauer.

Hoshi T, Zagotta WN, Aldrich RW (1990) Biophysical and molecular mechanisms of *Shaker* potassium channel inactivation. Science 250:533–538.

Jan LY, Jan YN (1997) Cloned potassium channels from eukaryotes and prokaryotes. Annu Rev Neurosci 20:91–123.

Kahn ES, Matsumoto H (1997) Calcium/calmodulin-dependent kinase II phosphorylates *Drosophila* visual arrestin. J Neurochem 68:169–175.

Kamb A, Iverson LE, Tanouye MA (1987) Molecular characterization of *Shaker*, a *Drosophila* gene that encodes a potassium channel. Cell 50:405–413.

Lichtinghagen R, Stocker M, Wittka R, Boheim G, Stuhmer W, Ferrus A, Pongs O (1990) Molecular basis of altered excitability in *Shaker* mutants of *Drosophila melanogaster*. EMBO J 9:4399–4407.

Matsumoto H, Kurien BT, Takagi Y, Kahn ES, Kinumi T, Komori N, Yamada T, Hayashi F, Isono K, Pak WL (1994) Phosrestin I undergoes the earliest light-induced phosphorylation by a calcium/calmodulin-dependent protein kinase in *Drosophila* photoreceptors. Neuron 12:997–1010.

Minke B, Selinger Z (1996) The role of TRP and calcium in regulating photoreceptor function in *Drosophila*. Curr Opin Neurobiol 6:459–466.

O'Day PM, Lisman JE, Goldring M (1982) Functional significance of voltage-dependent conductances in *Limulus* ventral photoreceptors. J Gen Physiol 79:211–232.

Pearson RB, Kemp BE (1991) Protein kinase phosphorylation site sequences and consensus specificity motifs, tabulations. Methods Enzymol 201:62–81.

Peretz A, Suss-Tobby E, Rom-Glas A, Arnon A, Payne R, Minke B (1994) The light response of *Drosophila* photoreceptors is accompanied by an increase in cellular calcium: effects of specific mutations. Neuron 12:1257–1267.

Perozo E, Bezanilla F (1990) Phosphorylation affects voltage gating of the delayed rectifier K^+ channel by electrostatic interactions. Neuron 5:685–690.

Pongs O (1992) Molecular biology of voltage-dependent potassium channels. Physiol Rev 72:69–88.

Pongs O, Kecskemethy N, Muller R, Krahjentgens I, Baumann A, Kitz HH, Canal I, Liamazares S, Ferrus A (1988) Shaker encodes a family of putative potassium channel proteins in the nervous system of *Drosophila*. EMBO J 7:1087–1096.

Ranganathan R, Malicki DM, Zuker CS (1995) Signal transduction in *Drosophila* photoreceptors. Annu Rev Neurosci 18:283–317.

Richard AR, Ghosh S, Lowenstein JM, Lisman LE (1997) Ca^{2+}/calmodulin-binding peptides block phototransduction in *Limulus* ventral photoreceptors: evidence for direct inhibition of phospholipase C. Proc Natl Acad Sci USA 94:14095–14099.

Roeper J, Lorra C, Pongs O (1997) Frequency-dependent inactivation of mammalian A-type K^+ channel KV1.4 regulated by Ca^{2+}/calmodulin-dependent protein kinase. J Neurosci 17:3379–3391.

Rudy B (1988) Diversity and ubiquity of K^+ channels. Neuroscience 25:729–749.

Salkoff L, Jegla T (1995) Surfing the DNA databases for K^+ channels nets yet more diversity. Neuron 15:489–492.

Salkoff L, Wymann R (1981) Genetic modification of potassium channels in *Drosophila* mutants. Nature 293:228–230.

Scott K, Sun Y, Beckingham K, Zuker SC (1997) Calmodulin regulation of *Drosophila* light-activated channels and receptor function mediates termination of the light response in vivo. Cell 91:375–383.

Scott K, Zuker C (1997) Lights out: deactivation of the phototransduction cascade. Trends Biochem Sci 22:350–354.

Singh S, Wu C-F (1989) Complete separation of four potassium currents in *Drosophila*. Neuron 2:1325–1329.

Soderling TR (1996) Structure and regulation of calcium/calmodulin-dependent protein kinases II and IV. Biochem Biophys Acta 1297:131–138.

Sumi M, Kiuchi K, Ishikawa T, Ishii A, Hagiwara M, Nagatsu T, Hidaka H (1991) The newly synthesized selective Ca^{2+}/calmodulin dependent protein kinase II inhibitor KN-93 reduces dopamine contents in PC12h cells. Biochem Biophys Res Commun 181:968–975.

Tempel BL, Papazian DM, Schwarz TL (1987) Sequence of a probable potassium channel component encoded at *Shaker* locus of *Drosophila*. Science 237:770–775.

Titus SA, Warmke JW, Ganetzky B (1997) The *Drosophila erg* K^+ channel polypeptide is encoded by the seizure locus. J Neurosci 17:875–881.

Tokumitsu H, Chijiwa T, Hagiwara M, Mizutani A, Terasawa M, Hidaka H (1990) KN-62, 1-[*N*,O-bis(5-isoquinolinesulfonyl)-*N*-methyl-L-tyrosyl]-4-phenylpiperazine, a specific inhibitor of Ca^{2+}/calmodulin-dependent protein kinase II. J Biol Chem 265:4315–4320.

Tsunoda S, Salkoff L (1995a) Genetic analysis of *Drosophila* neurons: *Shal*, *shaw*, and *Shab* encode most embryonic potassium currents. J Neurosci 15:1741–1754.

Tsunoda S, Salkoff L (1995b) The major delayed rectifier in both *Drosophila* neurons and muscle is encoded by *Shab*. J Neurosci 15:5209–5221.

Wang XJ, Reynolds ER, Deak P, Hall LM (1997) The seizure locus encodes the *Drosophila* homolog of the HERG potassium channel. J Neurosci 17:882–890.

Warmke J, Drysdale R, Ganetzky B (1991) A distinct potassium channel polypeptide encoded by the *Drosophila eag* locus. Science 252:1560–1562.

Weckstrom M, Hardie RC, Laughlin SB (1991) Voltage-activated potassium channels in blowfly photoreceptors and their role in light adaptation. J Physiol (Lond) 440:635–657.

Westphal RS, Anderson KA, Means AR, Wadzinski BE (1998) A signaling complex of Ca^{2+}-calmodulin dependent protein kinase IV and protein phosphatase 2A. Science 280:1258–1261.

Wickman KD, Clapham DE (1995) G-protein regulation of ion channels. Curr Opin Neurobiol 5:278–285.

Wu C-F, Ganetzky B (1992) Neurogenetic studies of ion channels in *Drosophila*. In: Ion channels, Vol 3 (Narahashi T, ed), pp 261–314. New York: Plenum.

Wu C-F, Haugland FN (1985) Voltage clamp analysis of membrane currents in larval muscle fibers of *Drosophila*: alteration of K^+ currents in *Shaker* mutants. J Neurosci 5:2626–2640.

Yellen G, Sodickson D, Chen T-Y, Jurman ME (1994) An engineered cysteine in the external mouth of a K^+ channel allows inactivation to be modulated by metal binding. Biophys J 66:1068–1075.

Zhong Y, Wu CF (1993) Modulation of different K^+ currents in *Drosophilia*: a hypothetical role for the Eag subunit in multimeric K^+ channels. J Neurosci 13:4669–4679.

Zuker SC (1996) The biology of vision in *Drosophila*. Proc Natl Acad Sci USA 93:571–576.